

Electroanalytical Evaluation of Antioxidant Activity of Cerium Oxide Nanoparticles by Nanoparticle Collisions at Microelectrodes

Naimish P. Sardesai, Daniel Andreescu, and Silvana Andreescu*

Department of Chemistry and Biomolecular Science, Clarkson University, Potsdam, New York 13699-5810, United States

S Supporting Information

ABSTRACT: We describe a simple, cost-effective and rapid electrochemical screening approach to evaluate antioxidant activity of cerium oxide nanoparticles (CeO₂ NPs) by single nanoparticle collision at microelectrodes. The method is based on direct monitoring of the interaction between a Pt microelectrode and surface bound superoxo and peroxy anions of CeO₂ NPs (CeO₂⁻/O₂²⁻) formed upon exposure to H₂O₂, selected here as a model reactive oxygen species. We observe an increase in spike current frequency for CeO₂ NPs exposed to H₂O₂, which we attribute to the reduction of surface bound oxygen species when the particles collide with the microelectrode. The results were confirmed with spectroscopic techniques that demonstrate changes in surface reactivity and composition. The spike frequency was found to correlate well with the superoxide dismutase activity of these particles. This approach could enable routine screening of antioxidant NPs using a rapid and inexpensive assay.

Applications of engineered nanoparticles (NPs) in electronics, catalysis, solid oxide fuel cells, medicine, electrochemistry, and sensing continue to increase.^{1,2} Traditionally, such NP systems are characterized by spectroscopic and microscopic techniques, such as TEM, AFM, EDS, X-ray photoelectron (XPS/ESCA), and XRD.^{3,4} These techniques are cumbersome and expensive which limit their routine use for screening purposes. Here, we report an electrochemical screening approach to assess activity of catalytically active antioxidant nanoparticles of (CeO₂) by measuring changes in their surface reactivity as they collide with a microelectrode.

CeO₂ NPs have received significant attention due to their catalytic and free radical scavenging properties, which made them attractive for multiple applications in biology, medicine, and catalysis.⁵⁻⁷ The presence of cerium in dual oxidation states on these particles (Ce³⁺/Ce⁴⁺) facilitates redox reactions at the particle surface, allowing them to react with reactive oxygen species (ROS) species and mimic activity of antioxidant enzyme systems, including superoxide dismutase (SOD) and catalase.⁸ Conventional methods to assess antioxidant activity involve complex procedures where enzymatic systems are used to generate radicals that are then detected by spectrophotometric and fluorimetric means using redox proteins or organic dyes.^{9,10} In these methods, light scattering and cross-reactivity of the particles with the redox components of the assay can affect accuracy of the analysis. NP collision electrochemistry at

microelectrodes is proposed in this work as an alternative approach to directly monitor antioxidant activity. This method can be particularly useful in the biomedical field for applications that require general assessment of the radical scavenging activity of these particles.

Electrochemical studies of NP collisions were first reported by Bard and collaborators to measure the transient current obtained by colliding Pt NPs with a carbon ultramicroelectrode (UME) in the presence of H₂O₂ or H₂ as indicators.¹¹ Compton and collaborators have monitored collision of Ag NPs with an immobilized electroactive molecule, *p*-nitrophenol and a glassy carbon electrode.¹² The resulting current was associated with the reduction of the redox adsorbed molecules on the Ag NPs surface. The profile and the magnitude of current–time (*i*–*t*) response reflected variations of size, agglomeration degree, and concentration of NPs. Previous studies demonstrated that the collision profile depends on the type of NPs and their surface coating, the indicator redox reaction, and the contact time between particles and electrode surface. A current ‘staircase’ response that increased in time was associated with NPs accumulation when the NPs stick successively on electrode surface after collision.¹¹ Such signals have been recorded at a carbon UME using Pt NPs for proton reduction or at an Au UME with Pt NPs for H₂O₂ reduction or hydrazine oxidation.^{11,13,14} A ‘spike’-like response was observed when the particles collide with the electrode surface. This response was attributed to the elastic collision between NPs and the electrode as the current decays to the background level when the NPs leave the electrode surface.^{15,16} Spike currents have been recorded for water oxidation with IrOx NPs at Pt UME,¹⁵ NPh reduction of *p*-nitrophenol-tagged Ag NPs at a glassy carbon electrode,¹² and for electrocatalytic oxidation of N₂H₄ at Hg-modified Pt UME.¹⁶ Until now, the utility of this technique has been limited to determination of particle size, shape, or concentration.

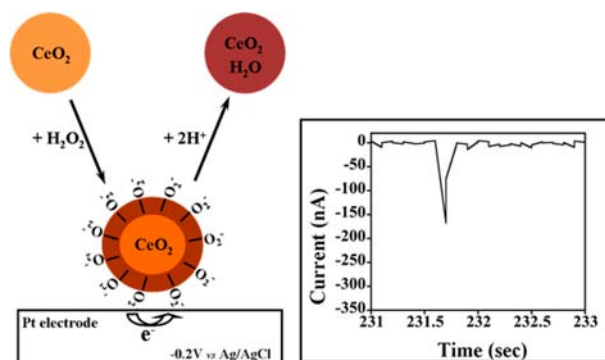
Here we evaluate the ability of the electrochemical collision technique to determine surface adsorbed species associated with oxidative damage by ROS and demonstrate the use of such measurements as a predictive screening tool of the antioxidant activity of CeO₂ NPs. Electrochemical collision signals of the NPs with a Pt microelectrode (PtME) are used to differentiate the reduced and unreduced forms of CeO₂ after exposure to ROS. Until now, monitoring ROS formation and inactivation was performed mainly by spectroscopic techniques. Herein we propose an electrochemical technique to quantify redox-induced surface changes as an indicator of the ability of these particles to

Received: August 5, 2013

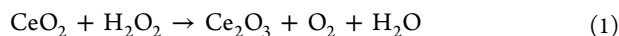
Published: September 30, 2013

bind and inactivate ROS. Exposure of CeO₂ NPs to ROS results in surface bound peroxo (O₂²⁻) and superoxo (O₂⁻)-like charge-transfer complexes of Ce–O₂⁻/O₂²⁻.^{17–19} O₂⁻/O₂²⁻ species can be monitored electrochemically at a Pt electrode at –0.2 V vs Ag/AgCl via the oxygen reduction reaction, where the O₂⁻ anion is an intermediate.²⁰ This process was used as an indicator reaction to detect the surface bound O₂⁻/O₂²⁻ on the CeO₂ NPs in the electrochemical collision process. Thus, experiments were conducted at an electrochemical potential of –0.2 V vs Ag/AgCl that corresponds to the reduction of the reactive O₂⁻/O₂²⁻. A NaBH₄ modified PtME ($\phi = 125 \mu\text{m}$) was used as the indicator electrode. Measurements were performed in nitrogen purged solutions with the bare and H₂O₂ exposed particles. The process is schematically represented in Scheme 1 which shows the collision generated response of the activated CeO₂ NPs at a PtME.

Scheme 1. Schematic Illustration of Single CeO₂ NP Collision Events and the Reduction Current Spike for the Ce–O₂⁻/O₂²⁻ NPs in Contact with The Pt ME ($\phi = 125\mu\text{m}$)



Single particle collision measurements with the PtME showed a number of spike-like electrochemical signals, which we attribute to the reduction of surface bound oxygen species, when the particles collide with the PtME with the CeO₂ NPs as a carrier. At the applied cathodic potential, electrons are injected to the surface adsorbed oxygen sites of the particle that comes in contact with the electrode. The process involves a series of sequential electron reduction reactions and may include adsorption, dissociation, charge transfer, and diffusion of these species to/from the activated particles to the PtME. Taking into account the redox process between CeO₂ and H₂O₂ (eq 1) and the transient nature of the surface adsorbed species, the current increase may be indicative of additional oxygen molecules generated by the reduced CeO₂ NPs close to the electrode surface as it reacts with H₂O₂ (eq 1) and by the reactive O₂⁻/O₂²⁻ anions adsorbed onto the NP surface as Ce–O₂⁻/O₂²⁻ complexes. These signals reflect the interaction of these particles with ROS.



To confirm the identity of the signal, CVs were recorded in PB in the absence and presence of CeO₂ NPs as controls and in the presence of the H₂O₂ treated CeO₂ NPs (Figure 1A). The CV of the blank sample in the absence of CeO₂ NPs showed a cathodic peak current corresponding to the four-electron oxygen reduction reaction on Pt (Figure 1Aa).²⁰ The intensity of this current decreased slightly with addition of CeO₂ NPs (Figure 1Ab). When identical tests were conducted with the H₂O₂ treated NPs, the intensity of the reduction peak current increased

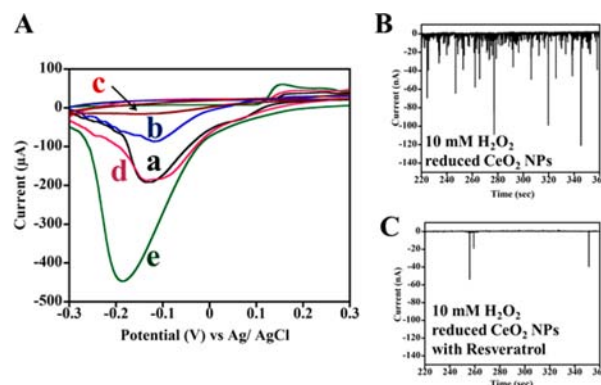


Figure 1. (A) CVs of PtME at a scan rate of 100 mV/s in absence of CeO₂ NPs (a) and presence of: CeO₂ NPs (b), CeO₂ NPs treated with 50 mM resveratrol (c), H₂O₂ reduced CeO₂ NPs treated with 50 mM resveratrol (d), and H₂O₂ reduced CeO₂ NPs (e). (B,C) Chronoamperometric plots of CeO₂ NPs. NP collisions for particles treated with 10 mM H₂O₂ (30 min) without (B) and with (C) resveratrol treatment. The collision experiments were performed at –0.2 V vs Ag/AgCl with N₂ purged 0.1 M PBS (pH 7.4) solution that contains CeO₂ NPs (4 mg mL⁻¹).

significantly with a slight shift toward a more negative potential of –0.2 V (Figure 1Ae). The specificity of the signal for the surface adsorbed oxygen species was assessed with a powerful antioxidant, resveratrol, that is known to have high inactivation behavior against ROS.^{21,22} Reduced CeO₂ NPs treated with 50 mM resveratrol showed significantly lower current intensity (Figure 1Ad) compared to that without resveratrol (Figure 1Ae). This indicates that ROS species formed on the reduced CeO₂ surface are responsible for the current enhancement. Similarly, an additional control experiment with the unreduced NPs showed decreased current in presence of resveratrol (Figure 1Ac).

Further experiments were conducted to study the particle collision profile and evaluate the analytical capabilities of the method. Electrochemical recordings provided a number of spikes at the applied potential of –0.2 V vs Ag/AgCl (Figure 1B). Few spikes with a very low current intensity, below 2 nA, were observed in the control experiment in the absence of particles (Figure 2). For quantification purposes only spikes with intensity above 10 nA were considered to differentiate between reduced and unreduced CeO₂ NP samples. We observed ~35(±4) spikes for bare CeO₂ NPs versus ~68(±5) spikes for the CeO₂ NPs that were exposed to 10 mM H₂O₂ for 30 min (Figure 2A) with good reproducibility for three independent measurements (Table S1). Conversely, the signals of the bare and activated particles exposed to resveratrol showed ~3(±1) spikes, which confirmed specificity of the spikes (Figures 1C and S1). To confirm that residual H₂O₂ did not contribute to the spike, a control experiment with the activated particles exposed to catalase was performed. Catalase is known to catalyze the decomposition of H₂O₂ to water and O₂. No significant difference in the CV or spike frequency was observed after treatment with catalase suggesting that residual H₂O₂ is not responsible for the observed signals (Figure S2). The few spikes recorded with bare CeO₂ NPs might indicate weakly physisorbed oxygen species present in the aqueous environment.²³ The significant difference in signal between the bare and the H₂O₂ treated CeO₂ NPs demonstrates that the electrochemical collision method is able to distinguish the reactivity of these particles against ROS. Such measurements can be used as a direct method to assess the antioxidant activity of these particles.

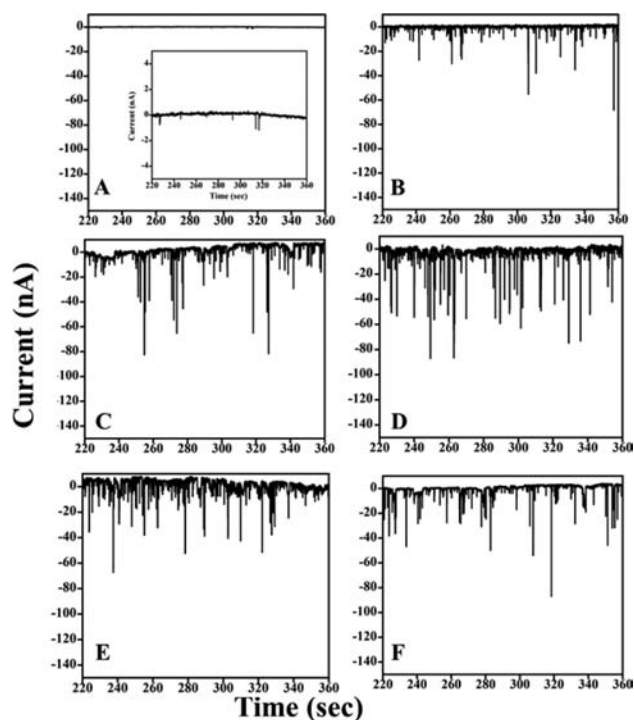


Figure 2. Chronoamperometric plots for CeO₂ NPs collisions at PtME in the absence of CeO₂ NPs (0.1 mM PBS alone) (A) and in the presence of untreated CeO₂ NPs (B), and CeO₂ NPs treated with different H₂O₂ concentrations of: 5 (C), 20 (D), 50 (E), and 100 mM (F) for 30 min. PBS containing CeO₂ NPs (4 mg mL⁻¹) was purged with N₂ for 20 min.

Different intensities may indicate differences in the size of colliding NPs in the colloidal dispersion. The shape of the current peak involves a fast current increase when a particular NP is in contact with the PtME and a slow current decay that can be attributed to loss of activity due to depletion of the redox species undergoing the electron transfer reaction. This time decay can differ from particle to particle due to variations in size and shape and can change the appearance of the spike. The commercial particles used in this study have particle sizes ranging between 10 and 20 nm and have variable shapes which may cause variations in current intensity. Similar observations with respect to intensity and shape of the spikes were reported for IrOx NPs collisions at Pt UME.¹¹ Typically, spike frequency was related to NPs concentration.^{11,16} Thus concentration of the redox adsorbed species on the H₂O₂ reduced CeO₂ NPs can be assessed by monitoring spike frequency, rather than the intensity and shape of the spike.

The impact of H₂O₂ concentration and exposure time on the frequency of the spike was further evaluated. These results were correlated with spectroscopic characterization of the NPs to further establish the origin of the spike and relate these signals to changes in the physicochemical and spectroscopic properties of the particles as they react with H₂O₂. Spikes increased in frequency for H₂O₂ concentrations up to 10 mM and decreased in frequency when the particles were treated with H₂O₂ concentrations from 20 to 100 mM (Figure 2). UV spectra of the particles treated with H₂O₂ in this concentration range showed the characteristic absorption peaks of CeO₂ NPs corresponding to the two oxidation states at 289 and 297 nm of Ce³⁺ and Ce⁴⁺, respectively.^{24,25} Details on the experimental procedure and results are provided in the SI. The Ce³⁺/Ce⁴⁺ ratio

(calculated from the specific absorbance intensities) increased within the first 30 min when the particles were exposed to 10 mM H₂O₂. Exposure times longer than 30 min decreased this ratio, indicating a reverse dismutation process (eq 2).⁸ For the same concentration range, the spike frequency increased when particles were treated with H₂O₂ for up to 30 min and nearly ceased when the exposure time was extended to 120 min (Figure S4). This trend accurately correlates with the UV data (Figure S3B) and suggests that the collision technique can also be used to study reaction kinetics of these particles.



Previous reports also found that CeO₂ NPs exposed to H₂O₂ concentrations in the 100 mM to 1 M range lost nearly all detectable SOD mimetic activity associated to the presence of Ce³⁺.¹⁹ Moreover, the presence of O₂⁻ on reduced ceria (Ce³⁺) was found to be energetically more favorable than on unreduced CeO₂ NPs (Ce⁴⁺).²³ Density functional calculations (DFT) also indicate that oxygen molecules interact with surface oxygen vacancies and Ce³⁺ ions that are in close proximity, resulting in fully oxidized Ce⁴⁺ and O₂⁻ bound species of charge transfer or electrostatic nature.²⁶ Thus the increase in the Ce³⁺/Ce⁴⁺ ratio and spike frequency for the H₂O₂ treated CeO₂ NPs can be attributed to the physisorbed O₂⁻ anion stabilized as a Ce–O₂⁻ complex. Moreover, in the aqueous environment the O₂⁻ anion can rapidly convert to peroxide O₂²⁻ type complexes, and thus both O₂⁻/O₂²⁻ could be expected. For H₂O₂ concentrations higher than 10 mM eq 2 is dominant favoring Ce⁴⁺.^{19,27} (Figure S3B, Table S3).

The presence of the surface adsorbed oxygen species onto the NPs surface was confirmed by FTIR spectroscopy, which revealed the enhancement of the O₂²⁻ stretching vibration (852 cm⁻¹) of surface adsorbed peroxo bonds in the sample treated with H₂O₂.²⁸ These bonds were significantly lower on the bare untreated particles. Additionally, the characteristic peak of the surface adsorbed O₂⁻ was seen in the 1100 cm⁻¹ region and that of adsorbed oxygen was observed at ~1600 cm⁻¹ in both control and treated particles (Figure S5). The TEM image of the particles showed highly crystalline CeO₂ NPs (25 ± 1 nm) with (111) lattice fringes of 3.12 Å (Figures S6C and S7). The XRD spectra showed broader XRD peaks for the CeO₂ NPs treated with 10 mM H₂O₂ as compared to the untreated particle suggesting structural changes in the crystalline structure of the particles exposed to H₂O₂ which might increase surface adsorbed oxygen species that lead to increase in spike frequency (Figure S6A and Table S4).

Since the spike frequency is related to the ability of these particles to bind and inactivate ROS, the collision frequency was further correlated with the superoxide inactivation ability of these particles (the SOD mimicking activity) determined using a conventional spectroscopic test, in which CeO₂ NPs replaced SOD (Table S5). The SOD mimetic assay is explained in detail in the SI. Figure 3 shows the correlation between the number of collisions and the superoxide inactivation % against the concentration of reduced CeO₂ NPs. Spike frequency varied linearly with the concentration of the reduced CeO₂ NPs, caused by the increase in the Ce-(O₂⁻/O₂²⁻) species (Figure 3, curve b). A similar linear relationship was observed for the O₂⁻ inactivation % that relates to the SOD mimicking activity as a function of CeO₂ NPs concentration (Figure 3, curve a). The results in Figure 3 demonstrate that it is possible to correlate NPs collision frequency to the superoxide inactivation activity of CeO₂ NPs. The chronoamperometric plots showed a clear

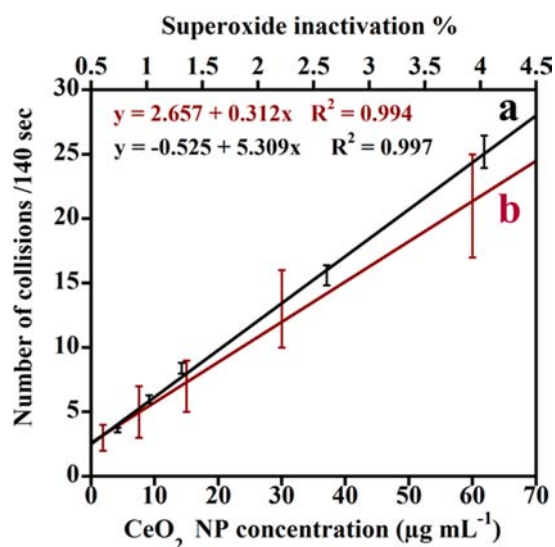


Figure 3. Correlation of the NP collision frequency as a function of O_2^- inactivation % (a) and concentration of treated CeO_2 NPs (b). CeO_2 NPs concentrations ranging from 1.875 to 60 $\mu\text{g}/\text{mL}$ were treated with 10 mM H_2O_2 for 30 min. PBS containing treated and untreated CeO_2 NPs (4 mg mL^{-1}) was purged with N_2 for 20 min.

difference in spike frequency for various commercial CeO_2 NPs (Figure S8). The results quantified as SOD equivalent units are in good agreement with the antioxidant activity assessed using conventional tests (Figure S9). This dependency can be used to assess and screen CeO_2 NPs for their catalytic activity against ROS based on their collision profile with a PtME after peroxide treatment. CeO_2 NPs are being tested in both animal and cell culture models to determine their ability to protect against oxidative stress.^{6,7,29} This method can be applied to screen particles for their ability to inactivate ROS and assist with prior selection of CeO_2 NPs candidates before more extensive cell and animal experimentation is being performed.

In conclusion, we demonstrated the use of the electrochemical NP collision technique to study fundamental surface properties of redox active CeO_2 NPs. We established a method that allows direct assessment of the antioxidant activity of these particles by NP collision experiments. We found that spike frequency increases due to increase of surface bound $\text{Ce}-\text{O}_2^-/\text{O}_2^{2-}$ species on CeO_2 NPs that come into contact with a PtME. Further we demonstrated that the antioxidant activity of CeO_2 NPs, as determined from the electrochemical collision data, is in agreement with that of a conventional detection method of the antioxidant activity. Fast screening of these particles can help in the identification of suitable NP candidates to be utilized in protection of cells against ROS and in drug delivery systems for the treatment of oxidative stress related diseases, such as recently reported applications to protect against ischemic stroke.⁶ This approach would bypass costly characterization techniques and enable routine study of these nanoparticles.

■ ASSOCIATED CONTENT

📄 Supporting Information

Experimental procedures and supporting figures. This material is available free of charge via the Internet at <http://pubs.acs.org>.

■ AUTHOR INFORMATION

Corresponding Author

eandrees@clarkson.edu

Notes

The authors declare no competing financial interest.

■ ACKNOWLEDGMENTS

This work was supported by grant NSF-1336493 to S.A. Any opinions, findings, and conclusions or recommendations expressed in this material are those of the author(s) and do not necessarily reflect the views of the National Science Foundation.

■ REFERENCES

- (1) Zhou, Z. Y.; Tian, N.; Li, J. T.; Broadwell, I.; Sun, S. G. *Chem. Soc. Rev.* **2011**, *40*, 4167.
- (2) Jiang, S. P. *Int. J. Hydrogen Energy* **2012**, *37*, 449.
- (3) Sharma, R.; Chee, S. W.; Herzog, A.; Miranda, R.; Rez, P. *Nano Lett.* **2011**, *11*, 2464.
- (4) Ziganshina, S. A.; Bizyaev, D. A.; Lebedev, D. V.; Chuklanov, A. P.; Bukharaev, A. A. *Russ. J. Appl. Chem.* **2010**, *83*, 1755.
- (5) Sun, C. W.; Li, H.; Chen, L. Q. *Energy Environ. Sci.* **2012**, *5*, 8475.
- (6) Kim, C. K.; Kim, T.; Choi, I. Y.; Soh, M.; Kim, D.; Kim, Y. J.; Jang, H.; Yang, H. S.; Kim, J. Y.; Park, H. K.; Park, S. P.; Park, S.; Yu, T.; Yoon, B. W.; Lee, S. H.; Hyeon, T. *Angew. Chem., Int. Ed.* **2012**, *51*, 11039.
- (7) Karakoti, A.; Singh, S.; Dowding, J. M.; Seal, S.; Self, W. T. *Chem. Soc. Rev.* **2010**, *39*, 4422.
- (8) Korsvik, C.; Patil, S.; Seal, S.; Self, W. T. *Chem. Commun.* **2007**, 1056.
- (9) Kalyanaraman, B.; Darley-Usmar, V.; Davies, K. J. A.; Dennery, P. A.; Forman, H. J.; Grisham, M. B.; Mann, G. E.; Moore, K.; Roberts, L. J.; Ischiropoulos, H. *Free Radical Biol. Med.* **2012**, *52*, 1.
- (10) Murrant, C. L.; Reid, M. B. *Microsc. Res. Tech.* **2001**, *55*, 236.
- (11) Xiao, X. Y.; Bard, A. J. *J. Am. Chem. Soc.* **2007**, *129*, 9610.
- (12) Zhou, Y. G.; Rees, N. V.; Compton, R. G. *Chem. Commun.* **2012**, *48*, 2510.
- (13) Xiao, X. Y.; Fan, F. R. F.; Zhou, J. P.; Bard, A. J. *J. Am. Chem. Soc.* **2008**, *130*, 16669.
- (14) Zhou, H. J.; Park, J. H.; Fan, F. R. F.; Bard, A. J. *J. Am. Chem. Soc.* **2012**, *134*, 13212.
- (15) Kwon, S. J.; Fan, F. R. F.; Bard, A. J. *J. Am. Chem. Soc.* **2010**, *132*, 13165.
- (16) Dasari, R.; Robinson, D. A.; Stevenson, K. J. *J. Am. Chem. Soc.* **2013**, *135*, 570.
- (17) Ornatska, M.; Sharpe, E.; Andreescu, D.; Andreescu, S. *Anal. Chem.* **2011**, *83*, 4273.
- (18) Ispas, C.; Njagi, J.; Cates, M.; Andreescu, S. *J. Electrochem. Soc.* **2008**, *155*, F169.
- (19) Heckert, E. G.; Karakoti, A. S.; Seal, S.; Self, W. T. *Biomaterials* **2008**, *29*, 2705.
- (20) Shao, M. H.; Liu, P.; Adzic, R. R. *J. Am. Chem. Soc.* **2006**, *128*, 7408.
- (21) Leonard, S. S.; Xia, C.; Jiang, B. H.; Stinefelt, B.; Klandorf, H.; Harris, G. K.; Shi, X. *Biochem. Biophys. Res. Commun.* **2003**, *309*, 1017.
- (22) Sharpe, E.; Frasco, T.; Andreescu, D.; Andreescu, S. *Analyst (Cambridge, U. K.)* **2013**, *138*, 249.
- (23) Choi, Y. M.; Abernathy, H.; Chen, H. T.; Lin, M. C.; Liu, M. L. *ChemPhysChem* **2006**, *7*, 1957.
- (24) Rao, G. R.; Sahu, H. R. *Proc. - Indian Acad. Sci., Chem. Sci.* **2001**, *113*, 651.
- (25) Yu, P.; Hayes, S. A.; O'Keefe, T. J.; O'Keefe, M. J.; Stoffer, J. O. *J. Electrochem. Soc.* **2006**, *153*, C74.
- (26) Preda, G.; Migani, A.; Neyman, K. M.; Bromley, S. T.; Illas, F.; Pacchioni, G. *J. Phys. Chem. C* **2011**, *115*, S817.
- (27) Scholes, F. H.; Soste, C.; Hughes, A. E.; Hardin, S. G.; Curtis, P. R. *Appl. Surf. Sci.* **2006**, *253*, 1770.
- (28) Li, C.; Domen, K.; Maruya, K.; Onishi, T. *J. Am. Chem. Soc.* **1989**, *111*, 7683.
- (29) Ganesana, M.; Erlichman, J. S.; Andreescu, S. *Free Radical Biol. Med.* **2012**, *53*, 2240.